Received: 24 February 2021 | Revised: 21 March 2021 | Accepted: 31 March 2021

DOI: 10.1002/jbio.202100068

JOURNAL OF BIOPHOTONICS

REVIEW ARTICLE

A review of specialty fiber biosensors based on interferometer configuration

Xuegang Li[1]* | Ning Chen[1] | Xue Zhou[1] | Pengqi Gong[1] | Shankun Wang[1] | Yanan Zhang[1] | Yong Zhao[1,2]

[1]College of Information Science and Engineering, Northeastern University, Shenyang, China

[2]Hebei Key Laboratory of Micro-Nano Precision Optical Sensing and Measurement Technology, Qinhuangdao, China

***Correspondence**
Xuegang Li, College of Information Science and Engineering, Northeastern University, Shenyang, Liaoning 110819, China.
Email: lixuegang@ise.neu.edu.cn

Funding information
China Postdoctoral Science Foundation; Fundamental Research Funds for the Central Universities, Grant/Award Number: N2004011; National Natural Science Foundation of China, Grant/Award Numbers: 61773102, 61903073, 61933004

Abstract

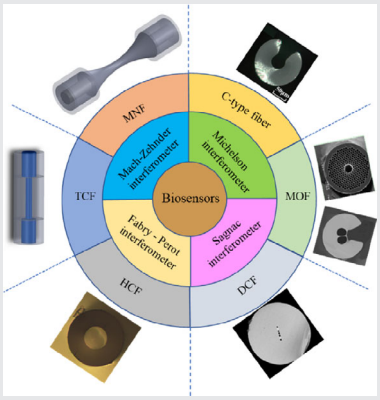

Optical fiber biosensors have attracted extensive research attention in fields such as public health research, environmental science, bioengineering, disease diagnosis and drug research. Accurate detection of biomolecules is essential to limit the extent of disease outbreaks and provide valuable guidance for regulatory agencies to take timely measures. Among many optical fiber sensors, optical fiber biosensors based on specialty fibers have the advantages of biocompatibility, small size, high measurement resolution, high stability and immunity to electromagnetic interference. In this paper, four types interferometer biosensors based on specialty fiber, namely Mach-Zehnder interferometer, Michelson interferometer, Fabry - Perot interferometer and Sagnac interferometer, are reviewed in terms of operating principles, sensing structure and application fields. The fiber types are further divided into micro-nano optical fiber, thin core fiber, polarization maintaining fiber, polymer fiber, microstructure optical fiber. Furthermore, this paper evaluates the advantages and disadvantages of these interferometer biosensors. Finally, main challenging problems and expectational development direction of specialty fiber interferometer biosensors are summarized. This text clearly shows the huge development potential of optical fiber biosensors in biomedical.

KEYWORDS

biosensor, DNA detection, interferometer, label free, optical fiber sensor

1 | INTRODUCTION

With the rapid development of biology, bio-sensing is important for many applications in public health research, environmental science, biological engineering, disease diagnosis and pharmaceutical research. At present, there are many methods for biosensing, such as optical, electro-chemical, thermometric, piezoelectric or magnetic. Among them, optical fiber biosensors have attracted wide attention because of their small size, superior biocompatibility and anti-electromagnetic interference characteristics and have been developing rapidly in

recent years. Kao KC found a glass fiber with a refractive index (RI) higher than its surrounding area [1]. With the development of optoelectronic technology [2], optical fiber has been deeply developed in various fields [3]. In medicine, optical fiber sensors are used to detect the presence or concentration of human biomass, such as DNA hybridization detection [4], *Escherichia coli* detection [5, 6], glutamic acid [7], acetic acid [8], antibiotics [9], cardiovascular diseases diagnosis [10]. In chemical detection, optical fiber is used to make chemical sensors, such as H_2S specific detection [11], NH_3 detection [12], ethanol concentration [13], harmful substances [14], urea [15], glucose [16, 17] and humidity [18]. The accurate detection of these biochemical molecules plays an important role in biomedical or clinical research. There is no doubt that optical fiber sensor has great development potential in biomedical or clinical research. [19].

Various methods for creating optical fiber biosensors have been proposed, such as fiber Bragg-gratings [20–25], long period fiber gratings [26], fiber interferometers [27–30], Brillouin/Raman scattering [31], surface Plasmon resonance [32–35], lossy-mode resonance [36], interferometer [37–41] and specialty fiber couplers [42]. Among them, the biosensors based on optical fiber interferometer are particularly attractive. Since the interferometer will provide a large amount of time and spectral information as its signal, it can quantitatively detect the measured object through a variety of methods, such as wavelength detection [43], phase difference [44], intensity [45], frequency [46]. With the help of these sensor indicators, it can be well applied in large dynamic range, high precision and high sensitivity sensing. Optical interferometry is a well-established technique for analyzing changes in optical thickness or RI and thus is a well-justified option for use in label-free biosensing. Due to the complexity and precision of biological organs, sensors used in biomedical or clinical research need to be miniaturized. The current trend of optical fiber interferometers is the application of micron level fibers. As a result, small optical fiber devices enable sensors to operate on a fiber scale [47]. As the effective choice for realizing miniaturized fiber interferometers, the in-line structure with two optical paths in one physical circuit has been extensively studied. The in-line structure has many advantages, such as easy alignment, high coupling efficiency and high stability [48]. At the same time, the optical fiber interferometer biosensor has the characteristics of simple design, ruggedness, portability, anti-EMI, shockproof and non-electrical operation. These are the functions required by any clinical diagnostic tool used in the hospital environment.

The optical fiber interferometer based on specialty fiber has received extensive attention due to its special structure and function [49, 50]. specialty fibers are the optical fibers with special designs or materials. In this paper, we only discuss silica fiber with special designs. Silica fiber has good biocompatibility thus is more suitable for biosensors. These specialty fibers include micro/nanostructured optical fiber (MNF), microstructured optical fiber (MOF), photonic crystal fiber (PCF) [51], polarization maintaining fiber (PMF), polymer fiber, hollow core fiber (HCF) [52], dual-core fiber (DCF). The interferometer based on specialty fiber has some advantages that other optical fibers do not have. For example, MOF can be filled with sensitive materials due to its unique air hole structure. [53]. In this way, closed measurement and high sensitivity measurement can be realized [54]. There are also advantages of MOF structure, such as wavelength free single-mode transmission, dispersion controllable, strong nonlinear effect, strong birefringence effect [55]. And these interferometer biosensors can be well applied in biomedical or clinical research due to their own advantages such as good biocompatibility.

This article aims to review and classify optical fiber interferometric biosensors with their principles, manufacturing methods of sensor probe and application fields. Due to the variety of sensing schemes, it is difficult to fully introduce all types of optical fiber biosensors in this review. Therefore, only specialty fiber interference biosensors are introduced.

2 | THE PRINCIPLE AND APPLICATIONS OF BIOSENSORS BASED ON SPECIALTY FIBER INTERFEROMETER

The famous Young double slit experiment was published in 1805 [56]. Young greatly promoted the development of light wave theory. Experiments have shown that light from a point light source passing through two closely spaced slits will produce an interference pattern at the terminal, which has been effectively used as a Young's interferometer in biosensor science [57]. In physics, interference is the phenomenon that two or more waves overlap in space, resulting in the formation of new waveforms. In this paper, four typical types of optical fiber interferometers are used to classify the biosensors of specialty fiber interferometers. They can be categorized into four types: Mach-Zehnder interferometer (MZI), Michelson interferometer (MI), Fabry - Perot interferometer (FPI) and Sagnac interferometer (SI).

For these four types of interference, the interference spectrum can be modeled by a simple two-mode interference equation,

$$I_{out} = I_1 + I_2 + 2\sqrt{I_1 I_2}\cos\varphi, \quad (1)$$

is the phase difference between them. When RI of the surrounding medium changes, the phase difference of the two beams will also change and the interference spectrum changes accordingly. The detected light signal can be demodulated to realize sensing. The majority of these interferometer configuration biosensors are based on the RI change induced by a molecular binding event on the sensor surface, which is directly related to the sample concentration. For example, the measurement of protein mainly depends on the combination of protein and protease to change the liquid RI. The measurement of DNA mainly relies on the combination of two complementary ssDNA to form double-stranded DNA to change the liquid RI. In general, most biomolecule measurements are due to the change of the RI of the liquid due to the combination of the test liquid and the functionalized film, which in turn causes the change of the spectral response. Thus, sensors with high RI sensitivity usually have high biological sensitivity after surface functionalization.

2.1 | Mach-Zehnder interferometer biosensors

2.1.1 | The principle of Mach-Zehnder interferometer

The basic structure principle diagram of optical fiber MZI is shown in Figure 1 and the basic principle is double beam interference principle [58]. The light is split into two beams via a coupler or splice point. A net phase difference is accumulated as the beams through the length of the fiber leading to Mach-Zehnder interference when the two beams are recombined.

2.1.2 | Mach-Zehnder interferometer biosensors based on micro/nanostructured optical fiber

MNF is a kind of specialty fiber with the diameter micron or even nanometer. MNF is widely used in detection, medical treatment, communication and other fields because of its high sensitivity. In 2015, Huang et al. presented a sensitive optical fiber biosensor based on a tapered fiber interferometer for in-situ detection of unlabeled single-stranded DNA (ssDNA) targets, as shown in Figure 2 [59]. The tapered fiber was coated with a high ordered pore arrays conjugated polymer to catch ssDNA. The polymer coating captures ssDNA molecules

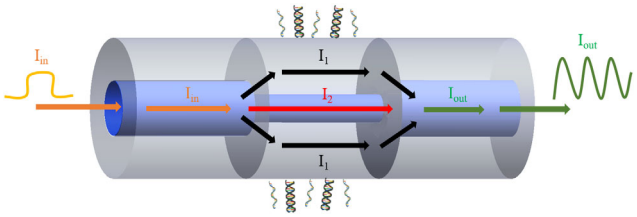

FIGURE 1 Structure diagram of typical fiber Mach-Zehnder interferometer

through π-π conjugate interaction and changes the surface RI of the tapered fiber, thus the output interference spectrum changes. Experimental results show the DNA concentration sensitivity of the sensor is 2.393 nm/log M and the minimum detection limit is 10^{-10} M or even lower.

Similarly, in 2016, Song et al. presented a label-free DNA biosensor based on the microfiber-assisted MZI for real-time detection of DNA hybridization kinetics [60]. Poly-L-lysine and probe ssDNA gradually form a sandwich coating on the surface of the tapered fiber, as shown in Figure 3. The interference transmission spectrum will change with the concentration and by using a U-shaped microcavity with a length of 176.88 μm, the detection limit is conservatively reduced to 0.0001 pmol/μL. The DNA biosensor proposed by this test has the advantages of small size, easy manufacture and strong reaction to DNA hybridization, which makes it well used in such aspects as medical diagnosis, cancer screening, drug inspection and environmental engineering.

In addition to DNA hybridization detection, MNF can also effectively detect other biological molecules and has broad application prospects. In 2016, Ding et al. presented a label-free micro-nano fiber interferometer biosensor for high-sensitivity detection of neurotransmitter molecules (5-HT) [61]. In the experiment, the fused biconical method was used to fabricate MNF and the silica nanospheres used in the experiment form a mesoporous structure on the surface of the fiber, so as to achieve the purpose of effectively collecting 5-HT molecules, as shown in Figure 4, the results show that the biosensor has a linear response with the sensitivity of 1.04 nm/log M in the concentration range from 100 fM to 1 μM. The method provided by this experiment has great benefits in many aspects including clinical diagnosis, biomedical engineering and nanotechnology.

In biomolecular detection, when the same sensor is used repeatedly, the maximum sensor intensity will gradually decrease (about 7.5% per cycle). Each time the functionalized microspheres are removed from the surface during the washing process, degradation of the

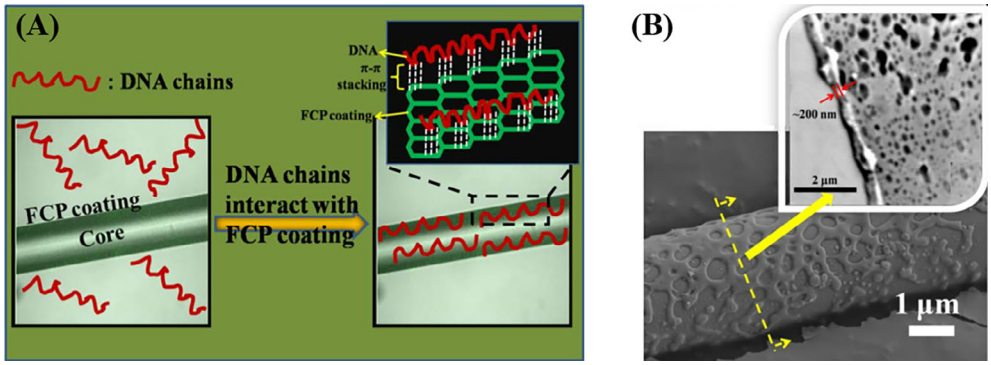

FIGURE 2 A, DNA strand and conjugated polymer coating interact through π-π stacking; B, Scanning electron microscope (SEM) image of the optical fiber surface [59]

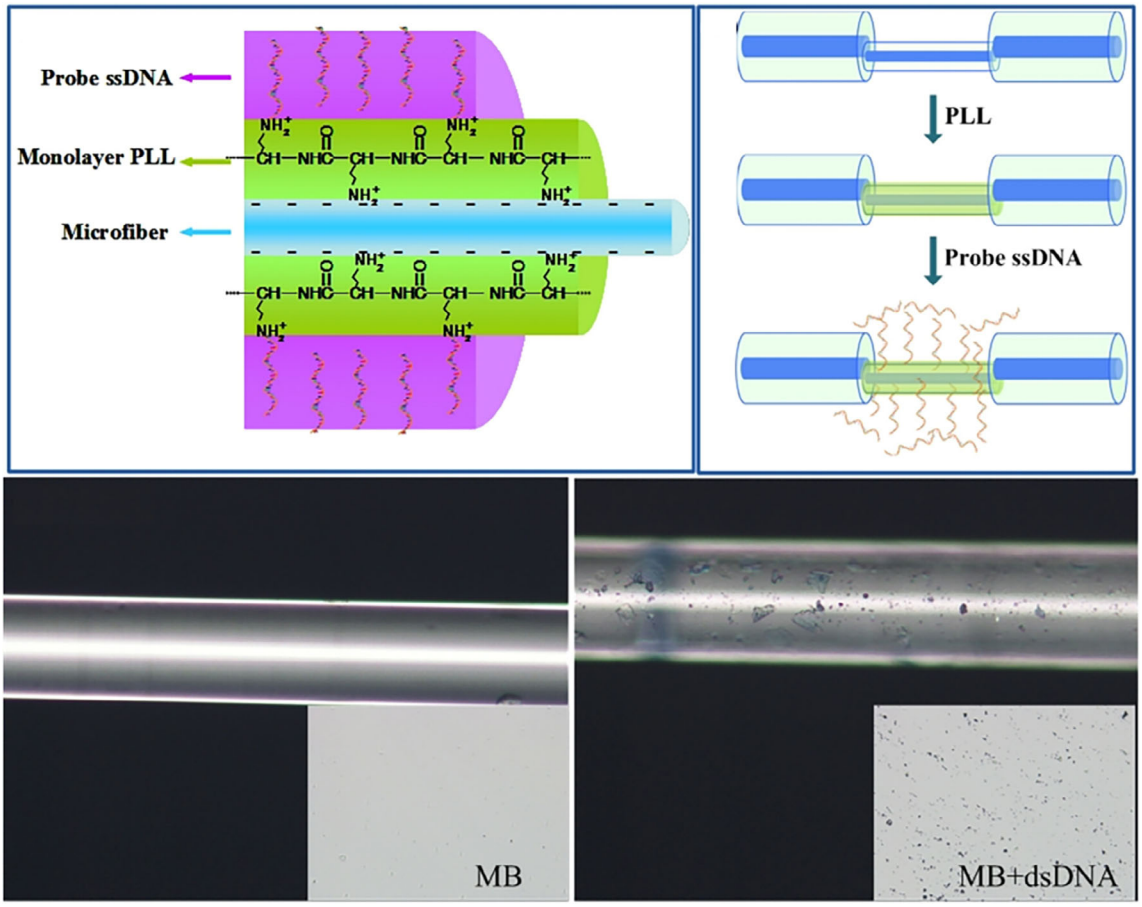

FIGURE 3 Stepwise functionalization procedure [60]

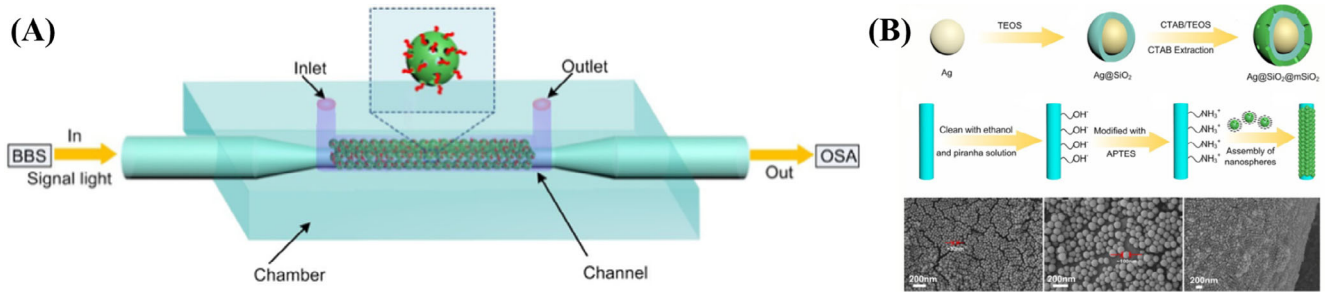

FIGURE 4 A, Experimental setup; B, Surface functionalization process [61]

sensor surface occurs. The microfluidic channel does not need to remove the microspheres, but is cleaned by the flow of cleaning fluid. So, the degradation can be reduced or avoided.

Using the same tapered fiber structure, by functionalizing the surface, Arjmand et al. reported a new optical biosensor for the detection of organophosphate compounds [62]. For methyl parathion, the concentration ranges from 10^{-10} M to 5×10^{-5} M and the detection limit of the biosensor is found to be as low as 2.4×10^{-10} M. The tapered fiber biosensor shows excellent repeatability for pesticides.

In addition to the detection of protein, MNF biosensor also realizes the measurement of some bacteria, such as the specific detection of *E. coli*. In 2018, Li et al. used multi-mode microfiber probes for fast response and label-free phage detection of *E. coli* [63]. Changes in the concentration of *E. coli* and the binding of the corresponding *E. coli* on the surface of the microfiber, as shown in Figure 5, will cause the shift of the wavelength, which can be used for biosensing research.

Experimental results show that the detection limit of the microfiber-based *E. coli* sensor is almost 10^3 cfu/mL compared with other works. Due to its advantages of high sensitivity and fast response, the microfiber fiber probes are excellently used in the fields of environmental monitoring and food safety.

For the MZI biosensors based on tapered MNF, its high fringe visibility, high sensitivity, small size and general assembly components have attracted extensive research and attention. However, there are still some shortcomings in MNF, because of its fragile sensing structure, it is easy to cause fiber fracture.

This section introduces the sensing performance, basic structure and functional method of MZI biosensors fabricated on MNF. Due to the ultra-small diameter and good biocompatibility of the micro-nano fiber, the sensor based on the micro-nano fiber has the basis for real-time monitoring in vitro, but it is necessary to solve the risk of the fiber being easily broken in the body.

2.1.3 | Mach-Zehnder interferometer biosensors based on microstructured optical fiber

MOF is a new type of fiber. Its core or cladding is no longer a single structure like the traditional fiber, but some micro-structures, such as periodic structure in the cladding and defect structure in the core, are introduced in it to obtain the performance different from that of the traditional fiber. MOF is very suitable for sensing because the characteristic longitudinal pores can act as tiny sample chambers and at the same time it can provide the effective RI required for light confinement [64]. Part of the guided light located in these holes can be used to generate effective modes required for many optical fiber sensing applications [65]. Unlike ordinary optical fibers, MOF can be made of a single material and has an appropriate cross-sectional design. This structure can provide most of the optical characteristics required by the sensor [66]. The optical fiber sensor made by the combination of traditional optical fiber and MOF has many excellent characteristics, such as filling characteristics, no cut-off high birefringence, single-mode transmission, adjustable dispersion [67].

In 2019, Hu et al. proposed a new type of liquid crystal biosensor based on optical fiber MZI [68]. Figure 6A depicts a schematic structure of the proposed biosensor. Figure 6B shows the cross section of the PCF, which cladding consist of air holes. The PCF is coated with 4′-pentyl-biphenyl-4-carboxylic acid mixed with 4-cyano-4′-pentylbiphenyl (5CB). The coating results are shown in Figure 6C.

At the same time, the experiment has obtained a local linear fit with a diameter of 50 μm and a pH range of 7.8 to 6.6. The pH measurement sensitivity is 1.21459 and R^2 is 0.97761. Therefore, the enzymatic reaction of penicillinase can be detected by monitoring the movement of the spectrum.

In addition to the measurement of pH by filling liquid crystal in PCF, the PCF sensor also realizes the rapid

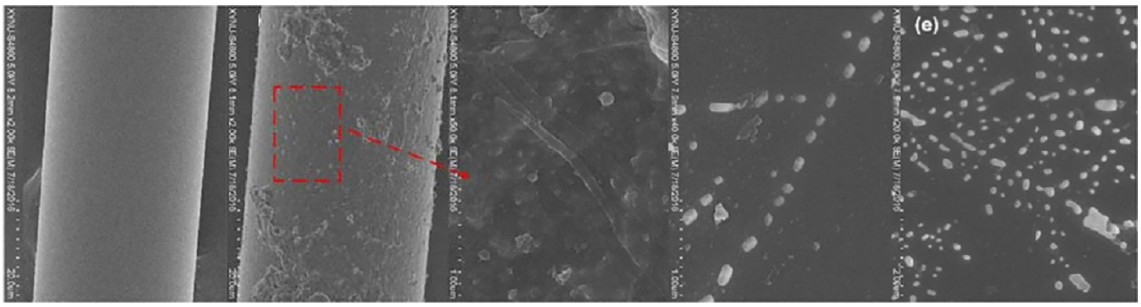

FIGURE 5 Scanning electron microscope micrograph of functionalized microfiber surface [63]

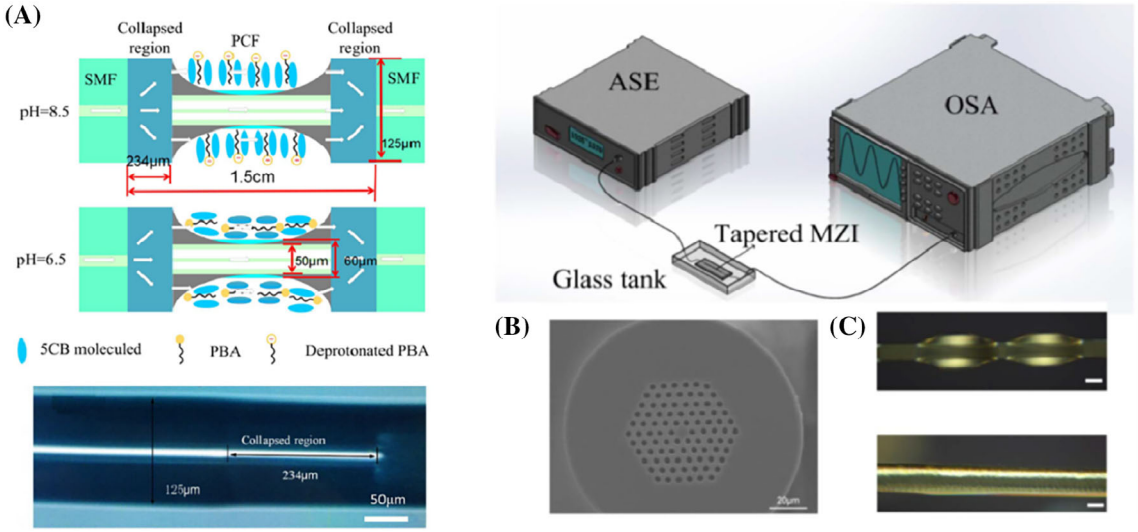

FIGURE 6 A, Schematic diagram of the sensing probe of 5CB doped PBA in Mach-Zehnder interferometer; B, Scanning electron microscope image of a photonic crystal fiber cross section; C, The coating results [68]

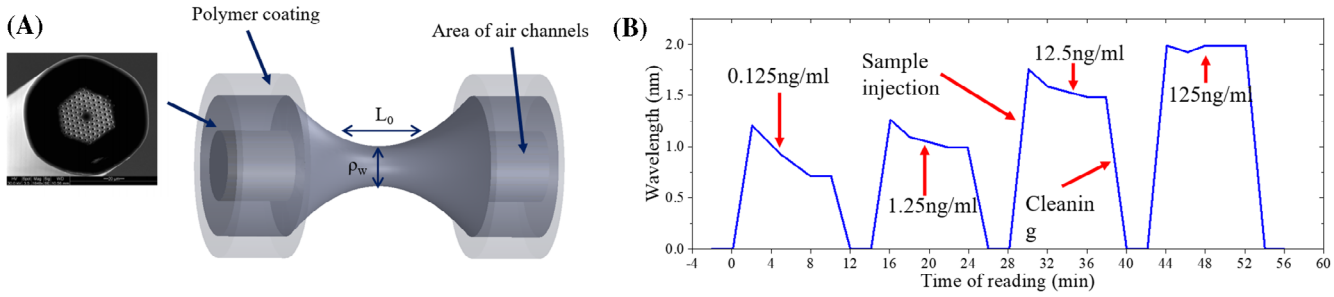

FIGURE 7 A, The scanning electron microscope of photonic crystal fiber (PCF) cross section (left) and diagram of tapered PCF (right); B, Sensor response with anti-BSA concentration between 0.125 and 125 ng/mL [69]

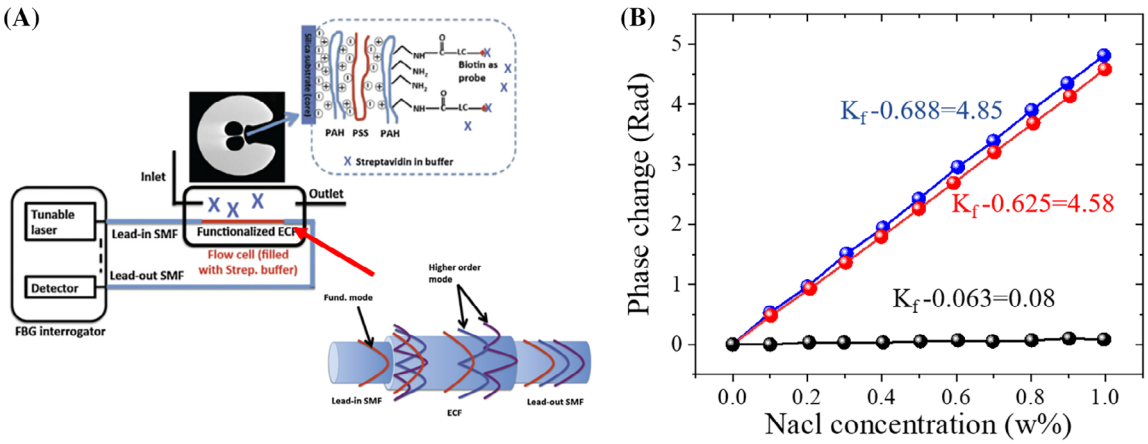

FIGURE 8 A, Schematic diagram of sensing system; B, Schematic diagram of phase change of experimental results [70]

detection of most antigens and antibodies. The same year, Vladimir P Minkovich et al. reported a non-adiabatic tapered PCF probe that can detect biomolecules, as shown in Figure 7 [69]. The experimental results show that the detection limit of Bovine albumin (BSA) antibody concentration is 125 pg/mL.

As a specialty fiber, exposed core fiber (ECF) is also a special MOF with two closed air holes and an open air-hole. It allows the external fluid to come into contact with the core of the ECF. At the same time, the core of this fiber allows multiple modes to spread. Due to the asymmetry of fiber structure, this fiber is also a birefringent fiber. According to the theory of evanescent wave, this kind of fiber will have higher RI sensitivity.

In 2015, Nguyen et al. presented a biosensor using multimode interference effect in ECF [70]. As shown in Figure 8A, biotin molecules are attached to the exposed surface of ECF to capture streptavidin. As shown in Figure 8B, when the highest intensity frequency of the spectrum is 0.625 nm^{-1}, the sensitivity is estimated to be 667 nm/RIU. The platform proposed in this experiment is feasible and provides a potential label-free biosensing detection method for clinical research.

The diversity of MOF structure makes it have some characteristics that ordinary fibers do not have. For example, the air hole structure of MOF makes it fillable. The RI sensitivity of the ECF can be significantly improved by the direct contact between the core and the external environment. In the clinical, this kind of sensor is more suitable for high sensitivity detection of some biomolecules in vitro due to the filling property and high sensitivity of the microstructural fiber. At the same time, due to the existence of microstructure fiber air space, the air hole can be used as a reaction container to achieve the mixing of multiple solutions to be tested, which also has a certain value in in vitro measurement.

2.1.4 | Mach-Zehnder interferometer biosensors based on thin-core fiber

TCF is a kind of specialty fiber, which has a core structure much smaller than ordinary optical fiber. The evanescent wave can easily reach the interface between the TCF and the environmental dielectric. Therefore, the good mechanical behavior of the optical fiber can be maintained without special treatment of the TCF [71].

In 2013, Yin et al. proposed a high-sensitivity optical fiber DNA sensor based on a thin-core fiber modal interferometer (TCFMI) [71]. Figure 9A shows the setup of DNA sensor testing based on TCFMI. As shown in Figure 9B, poly(ethyleneimine), poly (acrylic acid) and ssDNA are used to prepare polyelectrolyte multilayer membranes for DNA hybridization detection. As shown

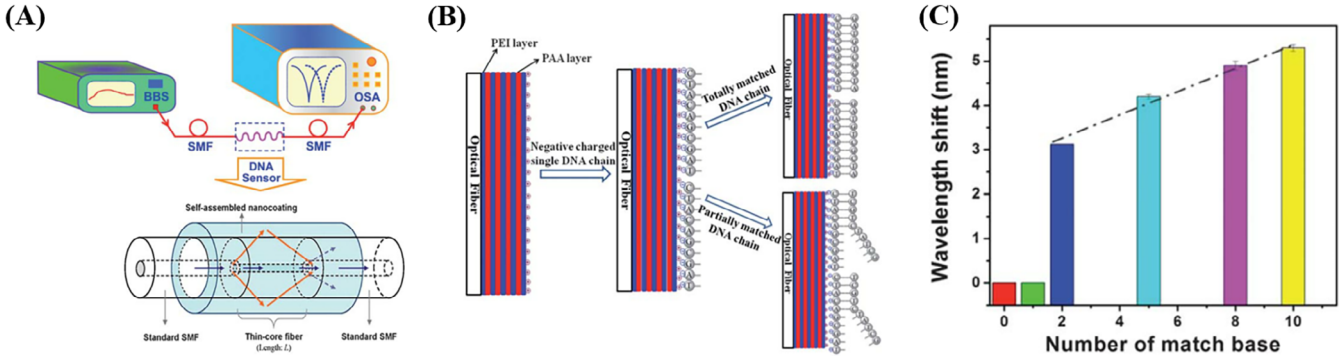

FIGURE 9 A, The setup of DNA sensor test based on thin-core fiber modal interferometer (TCFMI); B, The principle of a TCFMI-based DNA sensor; C, Experimental results of ssDNA detection of different targets based on TCFMI DNA sensor [71]

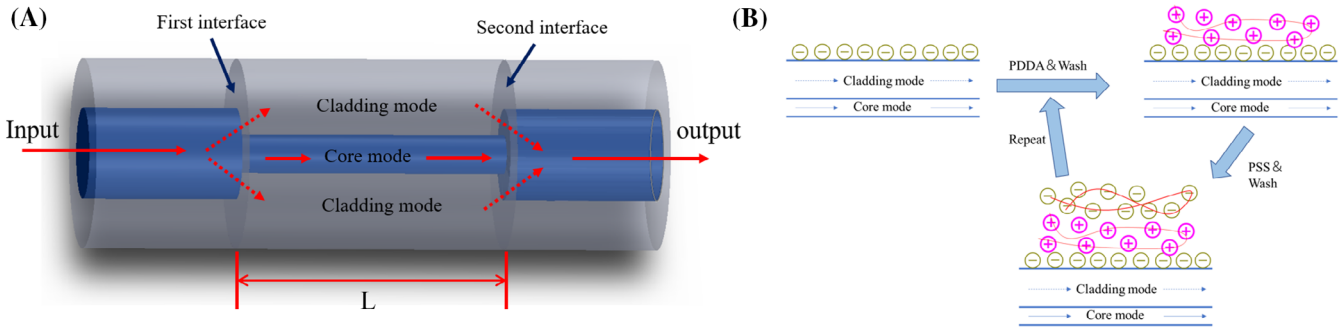

FIGURE 10 A, Schematic diagram of the sensing structure; B, polyelectrolyte self-assembled multilayers deposition process; C, Schematic diagram of spectral wavelength shift [72]

in 9(c), different types of target ssDNA solutions with a concentration of 1 mM were used in the experiment to test the fabricated DNA sensor. The results show that the sensitivity of the TCFMI-based ssDNA sensor at this concentration is 0.27 nm/matched base and can even detect the number of matched bases in the ssDNA strand.

Meanwhile, using the same structure, the surface functionalization shown in Figure 10B can be used to measure BSA. In 2016, Yu et al. realized the detection of protein by using SMF and TCF structure, As shown in Figure 10 [72]. The result showed that the detection limit was 0.02 nM. The experiment further verified the specificity of the structure by using BSA and gelatin. These results prove that the sensor can be used in biology and chemistry.

As a new type of optical fiber apparatus, the modular interferometer based on TCF has been widely concerned by researchers. The most studied structure is to weld a piece of TCF between two SMFs. Optical fiber devices made of thin core fiber usually show the advantages of low cost, compact structure, good robustness, high sensitivity to environmental parameters detection, anti-electromagnetic interference, so it has been widely used in many fields. This kind of sensor has high sensitivity and at the same time it solves the fragile problem of micro-nano fiber, which is also a solution for in vivo sensing.

MZI optical fiber sensor based on specialty fiber has a series of advantages. For example, biosensors based on MNF and TCF have high sensitivity, but also have the potential to achieve real-time measurement in vitro. Biosensors based on MOF with microfluidic channels provide a solution for the measurement of multi-component liquids. However, MZI interferometer is a transmission type interferometer, so biosensors based on this type of interferometer cannot achieve plug-in measurement, which is a major obstacle to the application of such sensors to in vivo measurements.

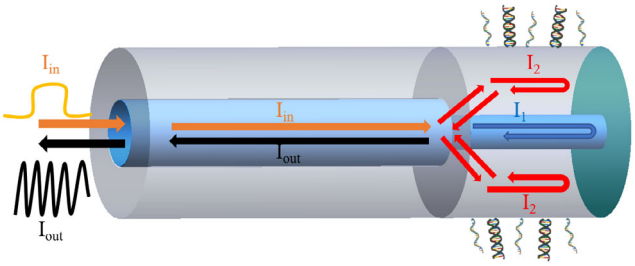

FIGURE 11 Structure diagram of typical fiber Michelson interferometer

2.2 | Michelson interferometer biosensors

2.2.1 | The principle of Michelson interferometer

Compared with the MZI, the MI adds a reflecting surface to the MZI in structure and observes not the transmission spectrum but the reflection spectrum [73]. The light is divided into two beams in the coupler and transmitted along the fiber and then reflected at the reflective end face of the fiber end, thus cause a Michelson interference

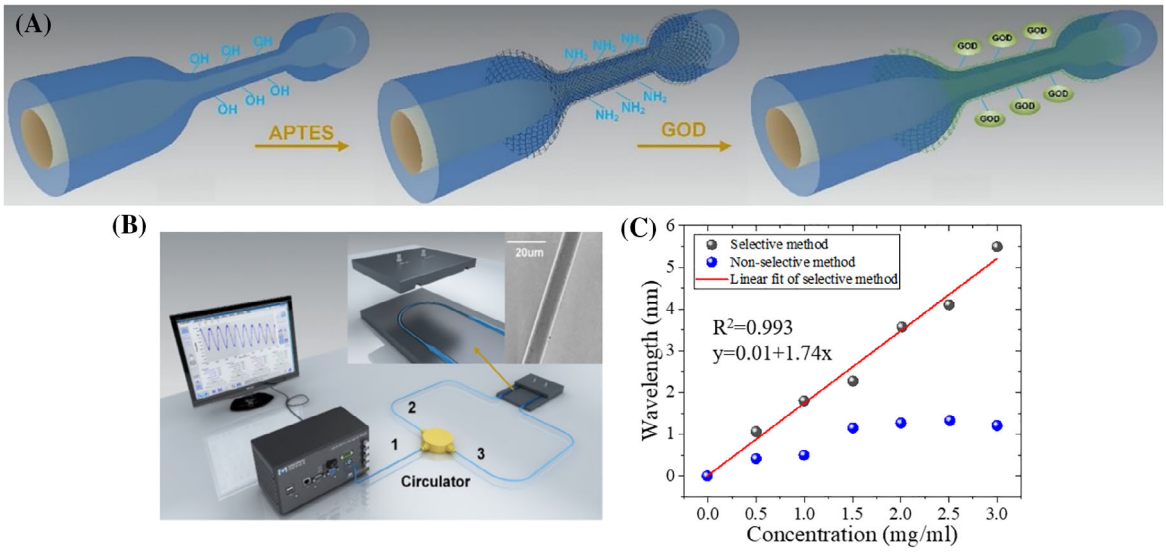

FIGURE 12 A, Functional schematic diagram of multimode tapered fiber; B, Experimental setup; C, Fitting graph of experimental results [76]

spectrum when the two beams are recombined in the coupler. The structure of the classic MI is shown in Figure 11.

Compared with MZI, MI sensor has become compact in structure and smaller in size. Parallel multiplexing of multi-sensor is another advantage of MI [74]. In terms of fabrication method, because of the similar structure, many manufacturing methods of MZI are also applicable to MI [75]. At the same time, it is easier to insert measurement due to its reflective structure.

2.2.2 | Michelson interferometer biosensors based on micro/nanostructured optical fiber

Similar to Section 2.1.2, MI can also be realized by using MNF. In 2018, Li et al. proposed an optical fiber biosensor functionalized with glucose oxidase (GOD) for the bioselective and highly sensitive detection of glucose [76]. As shown in Figure 12A, the experiment uses the free amine group of 3-aminopropyl-triethoxysilane (APTES) to fix the enzyme (GOD) on the tapered fiber probe through covalent interaction. As shown in Figure 12B, the tapered optical fiber sensor was immersed in glucose solutions of different concentrations and the experimental results were recorded. Experimental results show that the glucose concentration is linearly related to the resonance wavelength shift in the range of 0 to 3.0 mg/mL and the detection sensitivity is 1.74 nm/mg^{-1} mL^{-1}. At the same time, the sensor can accurately detect the glucose content in animal serum samples, which proves the practicability of the sensor.

2.2.3 | Michelson interferometer biosensors based on photonic crystal fiber

In 2010, Pawan et al. used a polymer nanoparticle composite film to enhance the evanescent field of the cladding mode, thus increasing the sensitivity of all-fiber MI

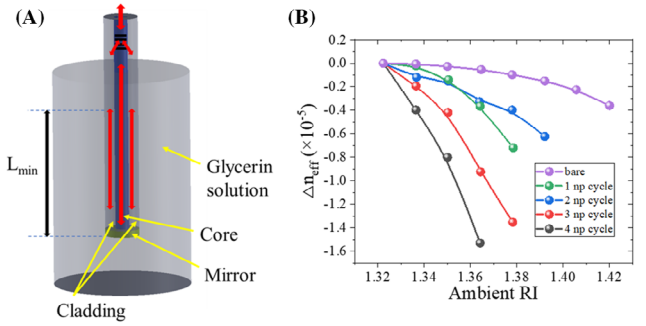

FIGURE 13 A, Diagram of an in-fiber MI; B, Experimental results [77]

to RI sensing [77]. As shown in Figure 13A, the use of layer-by-layer polyelectrolyte deposition and metal nanoparticle synthesis technology in the polymer composite film allows us to accurately form the thin RI coating required for the reorganization of the coating pattern. As shown in Figure 13B, the minimum detection limit is 3×10^{-3} RIU. As a high RI cover layer, polymer film also provides an ideal foundation for immobilization of biological reagents in biosensing applications.

In addition to using polymer nanocomposite film to improve the sensitivity of MI, MI can also be realized through other structures. In 2016, Gao et al. proposed an optical fiber biosensor to detect DNA hybridization and methylation, as shown in Figure 14 [78]. As shown in Figure 14C, the probe ssDNA is bound to the surface of the optical fiber through the poly-L-lysine layer and is detected by hybridization of the short probe ssDNA with the complementary target ssDNA. The reflection spectrum has edge visibility. Experimental results show that the detection limit reaches 5 nM.

The PCF biosensors based on MI have the advantages of high sensitivity, fast linear response and small volume. It simplifies the structure of MZI to some extent and makes it better used in biomedical.

2.2.4 | Michelson interferometer biosensors based on dual-core fiber

The DCF interferometer is not sensitive to temperature in a small range and has good linearity. So, it has potential application in biochemical sensing. However, the RI sensitivity is very high, so it can be used as an all fiber biochemical sensor.

In 2018, Wysokiński et al. presented an optical fiber protein sensor to achieve specific detection of specific proteins [79]. The results show that the optical fiber interferometer sensor detects the protein antigens in the solution by coating with specific antibodies. The wavelength shift measured by the spectrum analyzer or spectrometer can reach 0.6 nm. The detection system can be used as a template to detect various antigens, so it can be well used in medical diagnosis (Figure 15).

From the above examples, we can see that the optical fiber biosensors based on MI have the advantages of flexible structure, simple, easy to implement and can realize the parallel multiplexing of multi-sensor. Its good biocompatibility makes it widely used in biomedicine and other fields.

While MI biosensor has all the advantages of the MZI biosensor, it also adds the significant advantage of pluggable measurement, which lays a good foundation for the application of such sensors to real-time measurement in the body.

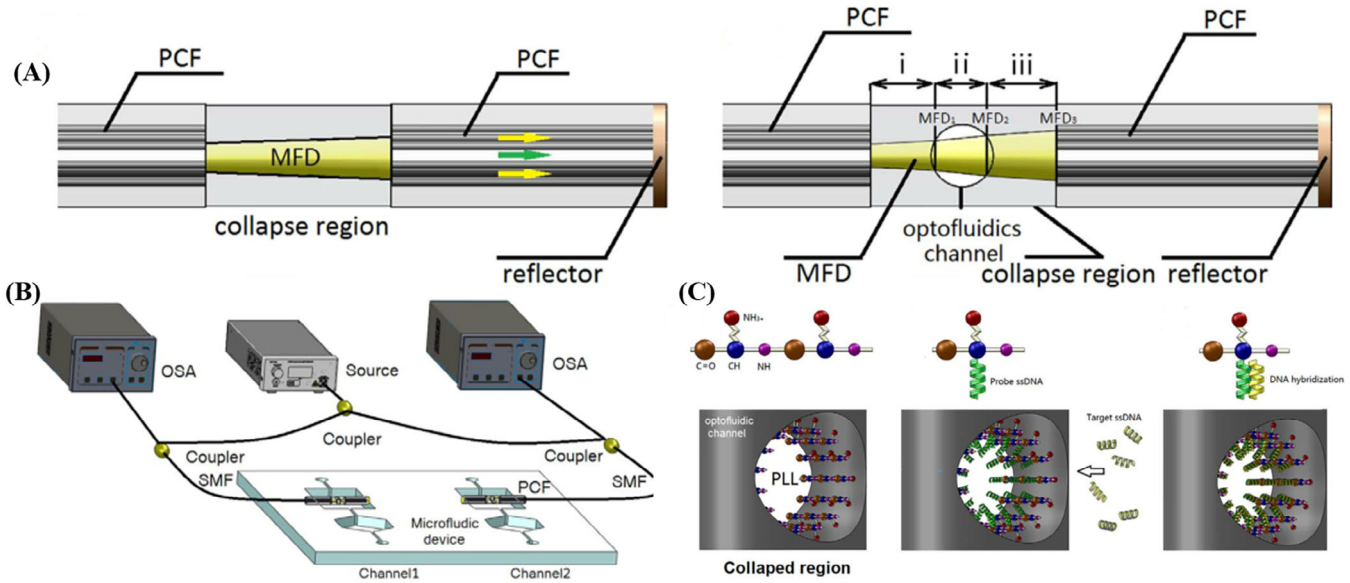

FIGURE 14 A, The schematic diagram of the photonic crystal fiber interferometric biosensor; B, Schematic diagram of experimental device; C, Surface functionalization process [78]

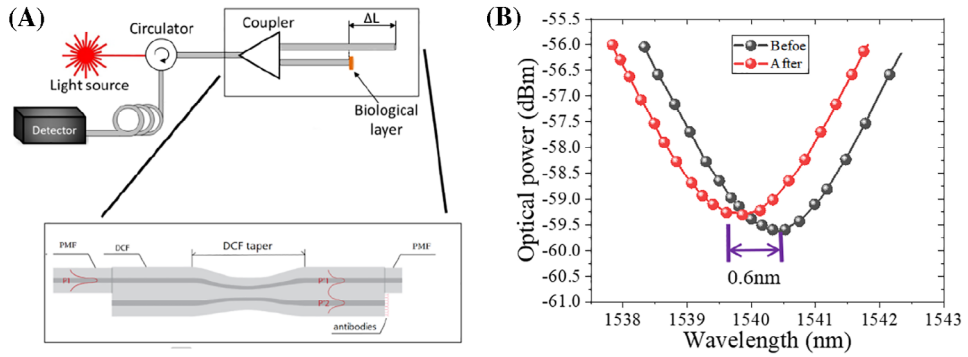

FIGURE 15 A, Monitoring system installation diagram; B, Wavelength shift of the optical fiber biosensor [79]

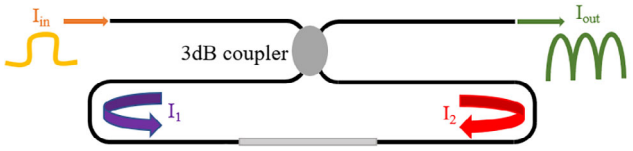

FIGURE 16 Structure diagram of typical fiber SI

2.3 | Sagnac interferometer biosensors

2.3.1 | The principle of Sagnac interferometer

The structure principle diagram of fiber SI is shown in Figure 16. Light from a broad-band source is split into clockwise and counterclockwise beams via a coupling zone as it enters the loop. A net phase difference is accumulated as the two polarization fundamental modes (ie, I_1 and I_2) through the length of the birefringent fiber, leading to Sagnac interference when the clockwise and counterclockwise beams are recombined at the coupling zone [80].

Compared with other interferometers, SI has the advantages of convenient manufacturing and strong environmental robustness [81]. However, it needs to form a loop, so it usually has a larger volume. Due to the ultra-high sensitivity of some SI, it has significant advantages for in vitro trace biological detection.

2.3.2 | Sagnac interferometer biosensors based on micro/nanostructured optical fiber

The combination of high RI sensitivity of SI and biosensing technology has great advantages in nucleic acid detection. In 2017, Gao et al. used the relative mode RI

change of the high birefringence (Hi-Bi) micro-nano fiber to propose a high-sensitivity, label-free optical fiber biosensor to specifically detect DNA molecules [82], as shown in Figure 17A. Compared with the traditional hybridization-based optical fiber acid sensor, this integrated biosensor has a 1000-fold increase in molecular sensitivity. As shown in Figure 17B, the target ssDNA concentration ranges from 100 pM to 1 μM and the detection limit is 75 pM. By modifying the sensor with conjugated polymer or graphene oxide, the functionalization efficiency can be further improved.

On the basis of one SI sensor, the cascade of two SIs is realized, which greatly improves the sensitivity of the sensor. In 2018, Wang et al. proposed a high birefringent microfiber biosensor based on the Vernier effect [83]. As shown in Figure 18B, the experiment uses two cascaded SIs to improve sensitivity. The experimentally measured RI sensitivity is 2429 nm/RIU. As shown in Figure 18B, the detection sensitivity of BSA can reach 9.097 nm/(mg × mL^{-1}). Experimental results show that the structure has the advantages of good biocompatibility and large specific surface area.

The sensitivity of traditional optical fiber biosensor is very limited. Because light is strictly confined to the core of the fiber, the interaction between light and biomolecules is limited. The sensitivity is further limited. The MNF biosensors based on SI can overcome these shortcomings and take advantage of its high sensitivity. This makes it brilliant in the field of biochemistry.

2.3.3 | Sagnac interferometer biosensors based on microstructured optical fiber

In 2017, An et al. proposed a compact glucose sensor using short length PCF [84]. Figure 19A shows an experimental setup for glucose detection using a PCF-based optical fiber SI sensor. As shown in Figure 19B, the RI response to glucose solution is achieved with a high average sensitivity of 22 130 nm/RIU and the glucose detection limit is 0.76 mg/dL, which is less than the effective detection line for hypoglycemia of 70 mg/dL. The simplicity of the fiber structure greatly reduces the production cost of the sensor.

ECF is a special type of MOF in which one side of the core is exposed to the surrounding medium. The open side causes an asymmetry in the fiber core, resulting in a birefringence effect. When the core is in direct contact with the object under test, the RI distribution becomes particularly asymmetric, so it can be effectively applied to biosensing [85].

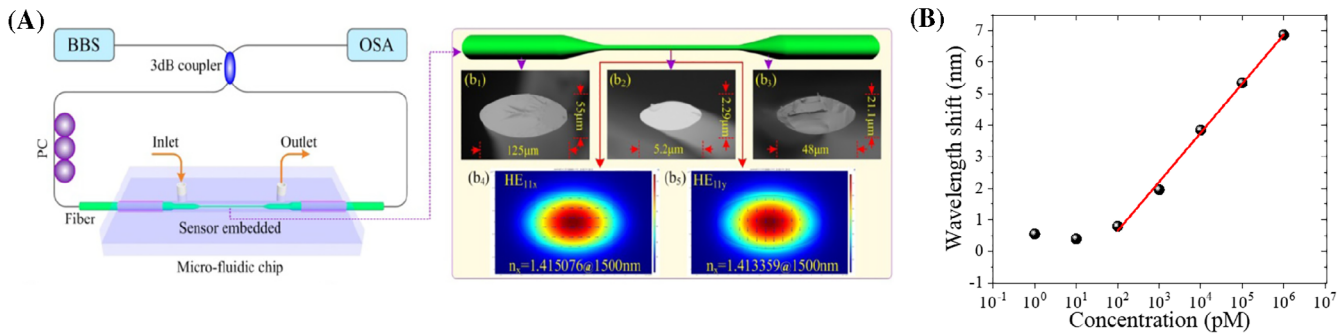

FIGURE 17 A, Schematic diagram of experimental setup; B, Experimental result spectrum; C, DNA hybridization test response [82]

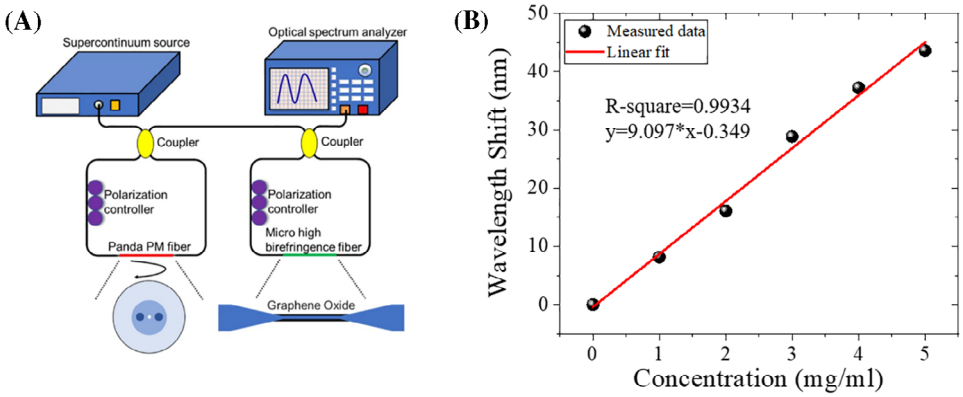

FIGURE 18 A, Schematic diagram of sensing system; B, The experiment of the cascaded SI loop to measure BSA solutions [83]

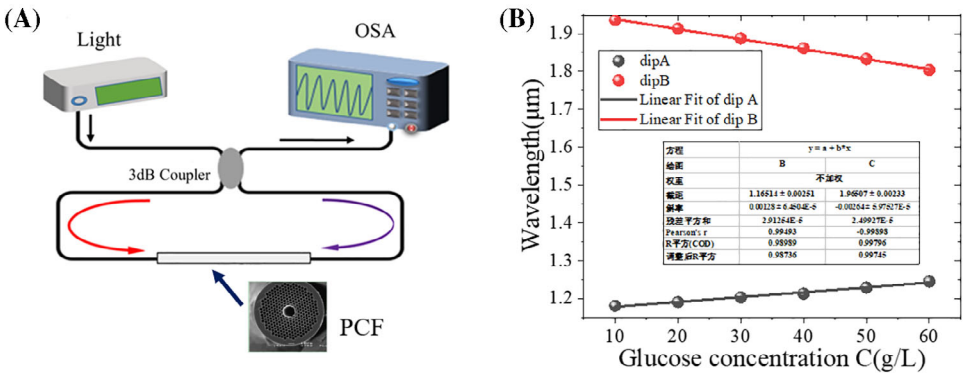

FIGURE 19 A, Experimental setup of the Sagnac interferometer; B, Fitting graph of experimental results [84]

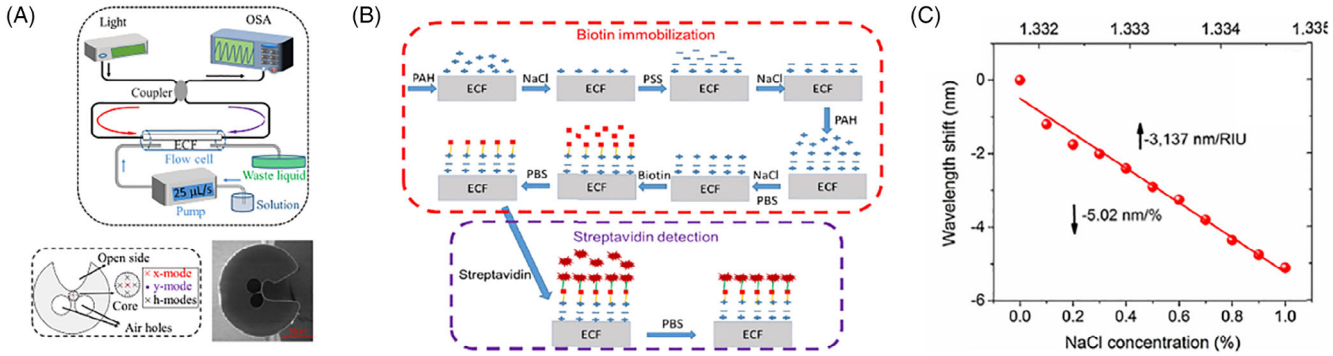

FIGURE 20 A, Schematic diagram of the sensing system; B, Detailed procedures of the surface-functionalization and biosensing; C, Fitting graph of experimental results [86]

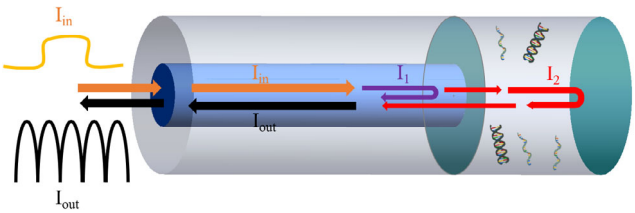

FIGURE 21 Structure diagram of typical fiber Fabry - Perot interferometer

In 2018, Li et al. presented a novel, high sensitivity SI biosensor based on ECF [86]. As shown in Figure 20B, the novel sensor uses biotin molecules to be immobilized on the surface of the ECF as capture probes to perform label-free detection of biomolecules for streptavidin detection. As shown in Figure 20C, the experiment measured that the sensor has an RI sensitivity of −3137 nm/RIU and the experiment proved that it can be used as a label-free biosensor.

SI has attracted great attention in various sensor applications due to its simple structure, easy fabrication and environmental robustness. In order to make full use of the polarization dependence of SI, birefringent fiber is usually used in the sensing part. However, in the measurement of biological parameters, due to its strong dependence on temperature, its high birefringence will reduce the sensing ability. In order to solve this problem, micro structured fiber is introduced as sensing fiber. The optical fiber SI sensor is a newly developed biomedical sensor, which has obvious advantages as a medical device.

As mentioned above, this type of sensor usually has a relatively large volume due to the need to form a ring and it is also unable to achieve insertion type in vivo measurement. However, due to its ultra-high sensitivity, this type of sensor has significant advantages for in vitro trace biological detection.

2.4 | Fabry - Perot interferometer biosensors

2.4.1 | The principle of Fabry - Perot interferometer

The concept of multi beam interference in optical fiber was proposed by Cielo et al. in 1979 [87]. This idea was implemented 2 years later by Petuchowski et al. The main structure of fiber FPI is an optical fiber interference

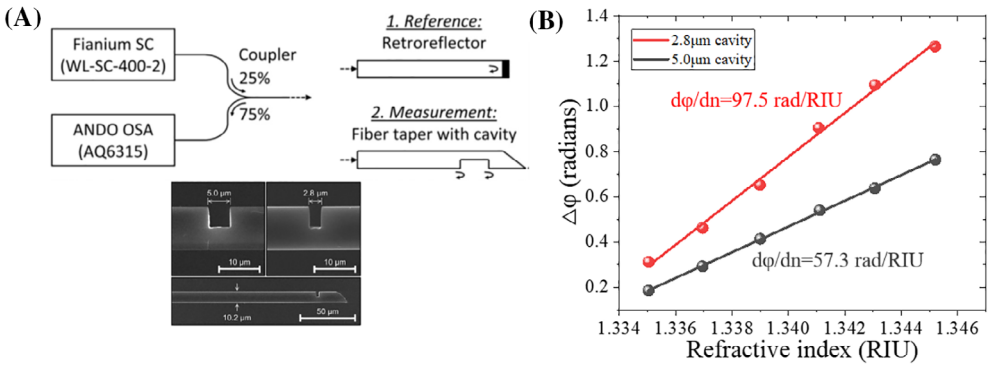

FIGURE 22 A, Schematic diagram of the optical measurement setup; B, Refractive index sensitivity fitting graph [89]

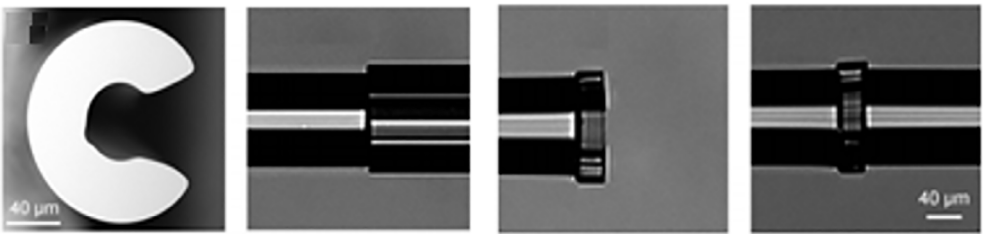

FIGURE 23 Fabrication process of the C-Fabry - Perot interferometer [90]

cavity [88]. The basic structure principle diagram of FPI is shown in Figure 21. The light is reflected at the two reflective surfaces, then FP interference occurs due to the existence of the optical path difference.

2.4.2 | Fabry - Perot interferometer biosensors based on micro/nanostructured optical fiber

In 2017, Smith et al. demonstrated the process of using focused ion beam milling to write ultra-small FPI cavities into optical microfibers [89]. As shown in Figure 22A, the test has produced a cavity as small as 2.8 m for sensing bulk RI and thin layer coating. In the center wavelength range of 610 nm, the estimated sensitivity of Figure 22B for a 5.0 μm cavity is 97.5 rad/RIU and the estimated sensitivity for a 2.8 μm cavity is 57.3 rad/RIU and the detection limit is on the order of 10^{-4}RIU. The detection limit of thin polymer coatings is on the order of 1 nm.

In the future, the sensor can add biochemical functions through polyelectrolyte coatings. For example, by appropriately attaching antibodies, specific detection of antigens can be achieved. The sensor system can also reduce costs and make it miniaturized.

MNF FPI sensor has been widely used for its high sensitivity and high precision. The optical fiber has excellent anti-EMI ability, which can monitor physiological acoustic signals in real time while using magnetic resonance imaging or other inspection procedures. Meanwhile, it is small and biocompatible, so it is safer for patients and easier to sterilize.

2.4.3 | Fabry - Perot interferometer biosensors based on C-type fiber

C-type fiber is a kind of specialty fiber with open side. As an open FP cavity, C-type fiber allows liquid samples to fill the gap between two SMFs. In 2014, Wu et al. presented an open cavity optical fiber FPI sensor by splicing a small piece of C-shaped optical fiber between SMFs, as shown in Figure 23 [90].The RI response of FPI is in the range of 1.33 to 1.36 and the RI sensitivity is 1368 nm/RIU at a wavelength of 1600 nm. Due to the all-glass structure of FPI, it has a very low temperature cross sensitivity of 3.04×10^{-7} RIU/°C.

Also using C-type optical fiber, in 2019, Xie et al. proposed a multi-parameter optical fiber sensor based on FPI, which is formed by continuous welding of C-shaped and single-mode optical fibers [91]. It realizes the measurement of biomolecules. The proposed sensor solves the dual-parameter problem in biochemical sensing and greatly reduces false positive measurements (Figure 24).

In addition to the measurement of Streptavidin, in 2020, Li et al. demonstrated an all-fiber all-optical qPCR system based on C-type fiber [27], as shown in Figure 25. In the paper, C-type fiber is used to construct the FPI and measure the temperature of the PCR mix in the cavity. The system can realize real-time and highly sensitive monitoring of fluorescence during the qPCR process. Experimental results show that the system can realize real-time fluorescence quantitative amplification of DNA and the platform technology may provide new strategies for basic technologies in biochemical applications, such as immediate care and remote diagnosis and on-site evidence collection.

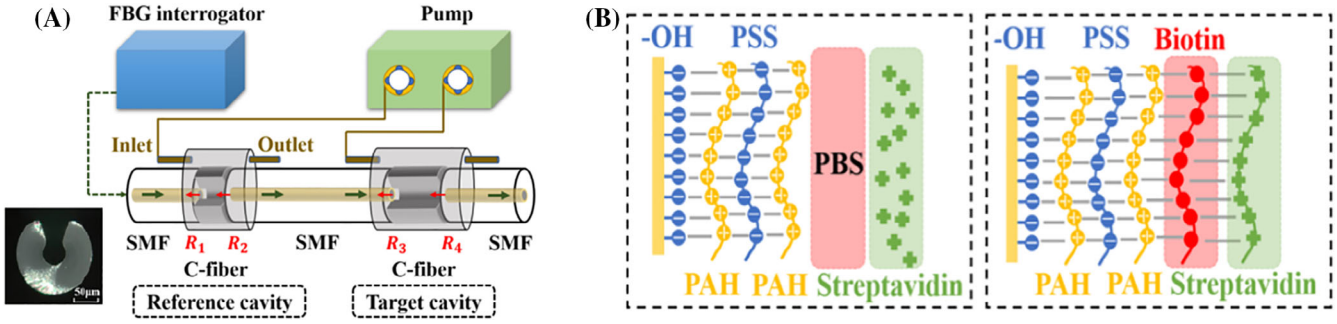

FIGURE 24 A, Schematic diagram of experimental device; B, Surface functionalization steps [91]

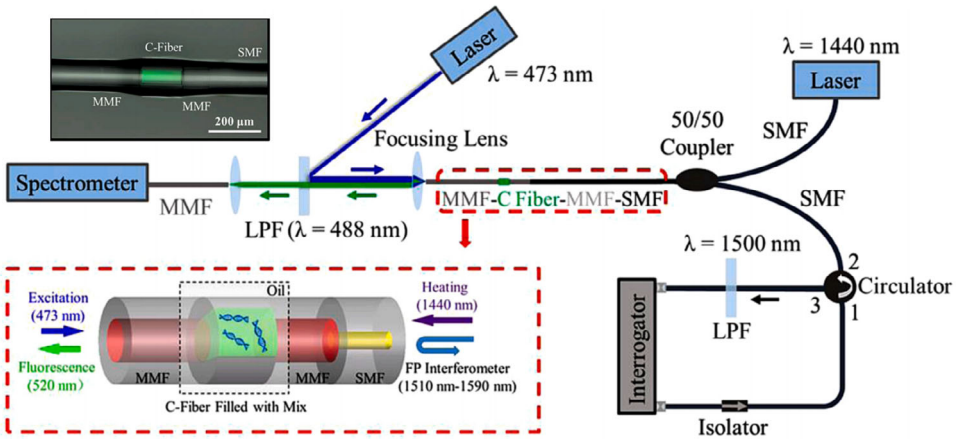

FIGURE 25 Schematic diagram of the all-fiber qPCR system [27]

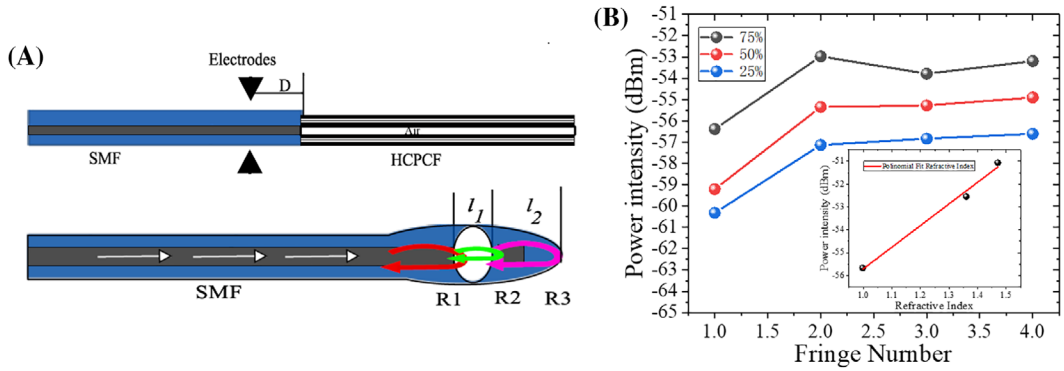

FIGURE 26 A, Experimental schematic; B, The sensitivity response [92]

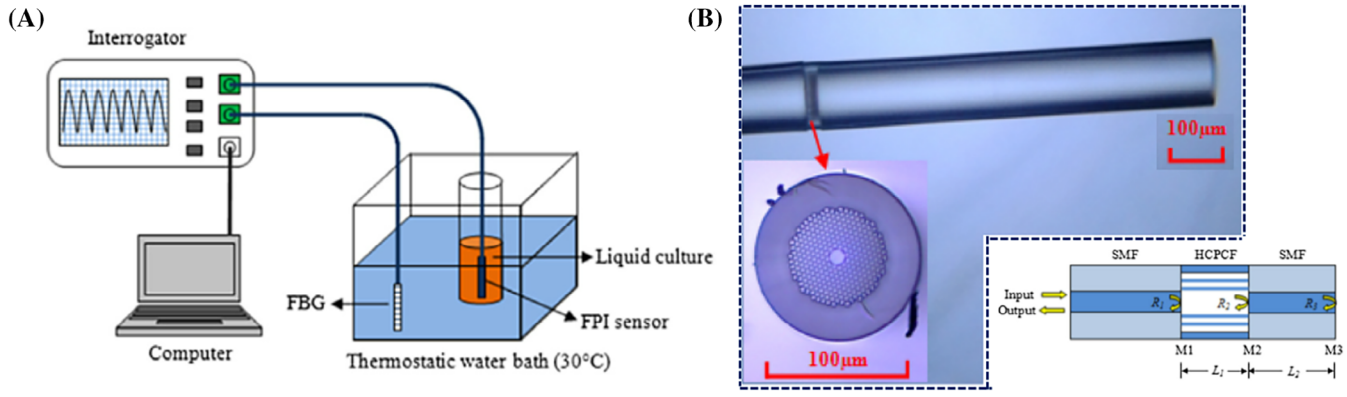

FIGURE 27 A, Experimental setup; B, scanning electron microscope micrograph of the Fabry - Perot interferometer optical fiber sensor [93]

The biosensor based on the C-type optical fiber has a high sensitivity because it has an open microfluidic channel that allows liquid to directly enter it. Meanwhile, the microcavity can be used as a microreactor. However, because the liquid directly participates in the optical path, this type of sensor usually has a large loss.

2.4.4 | Fabry - Perot interferometer biosensors based on microstructured optical fiber

PCF is also used in biosensor as a microstructure fiber. In 2013, Daniel et al. presented an intrinsic Fabry-Perot interferometer (IFPI) based on an air-microcavity [92]. As shown in Figure 26A, the air microcavity fused to SMF has a silica wall and is formed in a hollow photonic crystal fiber (HCPCF). As shown in Figure 26B, when the RI varies from 1 to 1.473, the measured fringe contrast changes about 4.7 dBm. The sensitivity to detect it can reach 9.94 dB/RIU.

Furthermore, the combination of PCF and SMF is used to improve the RI sensitivity of the sensor. In 2016, Liu et al. proposed a HCPCF-based optical fiber FPI for microbial growth detection [93]. Figure 27A shows the biosensing system. After the surface is functionalized, the sterile FPI sensor is vertically immersed in the liquid culture. The result shows that the yeast growth was successfully detected by the FPI sensor.

2.4.5 | Fabry - Perot interferometer biosensors based on hollow core fiber

In 2015, Zhang et al. designed a optical fiber sensor based on multi-cavity FPI [94]. The sensor achieves the measurement of surface functionalization of proteins such as immunoglobulin G (IgG) by measuring the thickness of self-assembled polyelectrolyte layers. For example, when the RI is assumed to be 1.432, the thickness change is 5.7 nm. The comparison of the optical thickness changes between different IgG bindings confirmed the specificity of the immunosensor (Figure 28).

By processing the top of the HCF, the purpose of biomolecule monitoring is achieved. In 2013, Chen et al. proposed a label-free optical fiber FPI immunosensor, which is realized by layer-by-layer self-assembly of chitosan and polystyrene sulfonate membrane suspended at the tip of HCF [95], as shown in Figure 29A. At the end of each immunoassay step, calculate and record the changes as shown in Figure 29B. The result shows that the sensor has the smallest response to unrelated anti-IgG, achieving a sensitivity of 0.033 μm/(pg/mm^2) and a detection limit of 0.005 nM.

In short, part of the external FPI optical fiber sensor is made of hollow fiber and fiber lens, which has a simple structure and accurate measurement. It can be used for real-time RI measurement of various liquid and protein samples and other biosensors.

Compared with MZI, MI and SI sensors, FPI based biosensor has an ultra-small volume and the length only needs to be tens of microns or even a few microns, so it is very suitable for inserting measurement. In addition, because of its microcavity, the microcavity can be used as a microreactor, for example, PCR amplification can be achieved. At the same time, because the microcavities can be cascaded, this type of sensor can theoretically realize simultaneous measurement of multiple biomolecules.

3 | STATUS AND COMPARISON OF BIOSENSORS BASED ON SPECIALTY FIBER INTERFEROMETER

Table 1 shows a summary of the specialty fiber interferometer sensors. As shown in Table 1, We give the classification of four kinds of interferometer sensors according to the category of optical fiber. The optical fiber interferometer sensor has achieved most of the biomass measurement and achieved good experimental results. Those sensors have the advantages of good biocompatibility, label free and real-time measurement. The MI and FPI have a smaller size compared with MZI and SI. At the same time, due to the reflective structure of these two interferometers, they have the potential of inserting in-

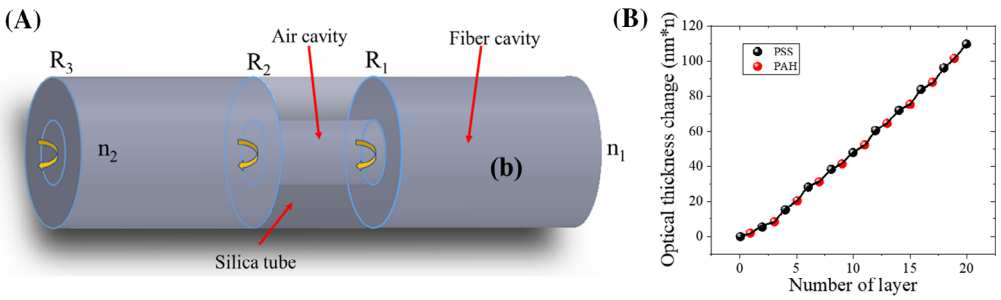

FIGURE 28 A, Structure of the multicavity Fabry - Perot interferometer sensor; B, The increase in the number of polymer layers leads to an increase in optical thickness; C, Optical thickness change diagram of fiber membrane cavity [94]

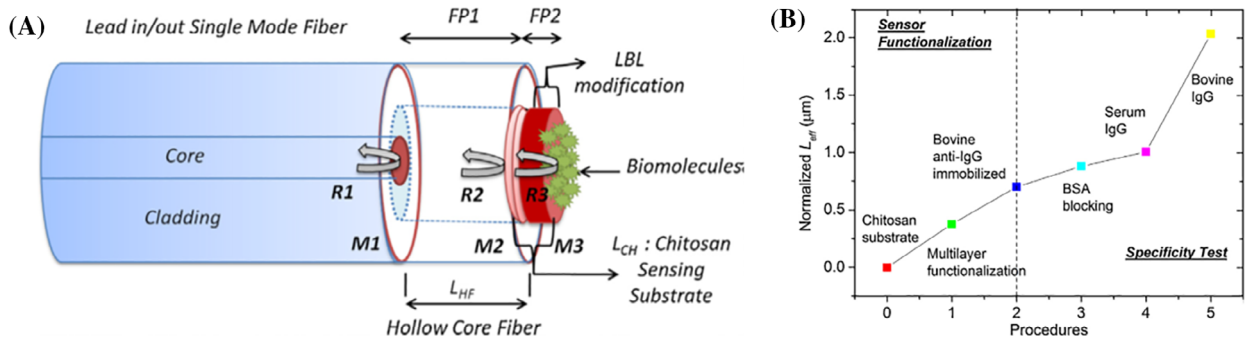

FIGURE 29 A, Sensor structure diagram; B, Response of each experimental step [95]

TABLE 1 Overview of specialty fiber sensors with different interferometer

Principle	Fiber type	Sensitivity	Advantage	Disadvantage	Reference
Mach-Zehnder	MNF	2.393 nm/log M	High sensitivity, superfine diameter.	Fragile structure, poor repeatability, temperature cross interference and transmissive structure	[59]
		1.04 nm/log M			[60]
	MOF	667 nm/RIU	High sensitivity, strong structure.	Complex optical fiber manufacturing method, transmissive structure	[67]
		1.21459 nm/pH			[69]
	TCF	0.55 nm/(ng/mm^2)	Easy to make and strong structure.	Low sensitivity and temperature cross interference	[72]
Michelson	MNF	1.74 nm/(mg^{-1} mL^{-1})	Small size, reflection-type probe structure and high sensitivity.	Fragile structure, poor repeatability and temperature cross interference	[76]
	PCF	7253 dB/RIU	Small size, reflection-type probe structure, high sensitivity.	Complex optical fiber manufacturing method	[77]
	DCF	High			[79]
Sagnac	MNF	13 488 nm/RIU	Ultrahigh sensitivity, superfine diameter.	Fragile structure, larger size, poor repeatability, circle structure and temperature cross interference	[82]
		9.097 nm/(mg·mL^{-1})			[83]
	MOF	22 130 nm/RIU	Ultrahigh sensitivity.	Complex optical fiber manufacturing method	[84]
Fabry-Perot	MNF	97.5 rad/RIU	Ultra-small size, reflection-type probe structure, high sensitivity, can be cascaded.	Difficult to manufacture, poor repeatability	[89]
	MOF	136 dB/RIU			[93]
	HCF	0.033 μm/(pg/mm^2)			[95]

body real-time measurement. In addition, because the microcavities can be cascaded, FPI based sensor can theoretically realize simultaneous measurement of multiple biomolecules. The interferometers based on MNFs has high sensitivity, but they have fragile structures and they are affected by temperature cross sensitivity. This type of sensor has significant advantages for in vitro trace biological detection. The interferometers based on the MOFs have the advantages of high sensitivity, but they suffer the more complex fabrication process. In addition, due to the existence of air holes or micro flow channels, MOF can be used as a micro reaction chamber, such as qPCR system. Sensors based on amplitude demodulation are easily affected by the external environment, resulting in noise and light loss, thus the demodulated result is difficult to achieve effective biomass measurement. However, sensors based on phase and wavelength have better ability to resist environmental interference. At the same time, it has the advantage of high demodulation accuracy.

All of those optical fiber biosensors have good label-free and specificity. At the same time, repeatability is also

an important factor of biosensors. For optical fiber DNA biosensors, the DNA double-strands can be separated by high-temperature heating, thus optical fiber DNA biosensors normally have a good repeatability. However, for some protein sensors, the protein is combined with the protease on the surface of the optical fiber to form a new substance, which is not reversible and thus not reproducible. Therefore, the repeatability of the optical fiber is closely related to the functionalized film of the optical fiber biosensors. About the ability to resist temperature interference, optical fiber biosensors normally have a weak resistance to temperature interference. There are two main reasons for this. First, the RI of the optical fiber material (SiO_2) is affected by temperature variations due to thermo-optic effect and thermal expansion effect. However, due to the mono-material nature of MOF, the MOF itself is slightly better at resisting temperature interference than other types of optical fibers, such as MNF, TCF and DCF. Second, almost all of the label-free, specific-detection optical fiber biosensors are based probe-target biological binding. However, their sensitivity of biomolecule detection is influenced by temperature tremendously [96] due to the insufficient bond of target molecule and probe molecule at non optimal temperature [97, 98]. Therefore, most biological experiments require real-time temperature monitoring.

However, the existing optical fiber biosensors are normally used in laboratory environments, successful commercial applications are a challenge, which also is one of the goals in the future. In practical applications, there are many types of biomass, so it is necessary to measure multiple biomolecules at the same time, which has also attracted much attention in recent years. In addition, high sensitivity has always been the goal of sensor researchers. At the same time, the response time and reuse of sensors are also future development goals.

4 | CONCLUSIONS

In this paper, the research progress of biosensors based on specialty fiber interferometer is reviewed. We introduced the working mechanism and biosensing principle of MZI, MI, SI and FPI optical fiber systematically. Based on the classification of specialty fiber types, the biosensors of specialty fiber interferometer are reviewed in detail. The main specialty fibers include MNF, TCF, PMF, POF and MOF. Finally, by summarizing the existing shortcomings and future needs of optical fiber interferometer sensors to predict its future trends. The examples fully verify that specialty fiber biosensors based on interferometers have been widely used in biomedical in the laboratory and show the potential prospects for clinical area. The sensor has good sensitivity, response time and biocompatibility, but the repeated use and potential insert in vivo testing of the sensor need to be improved.

ACKNOWLEDGMENTS

This work was supported by China Postdoctoral Science Foundation; the National Natural Science Foundation of China under grant (61903073), (61933004) and (61773102); The Fundamental Research Funds for the Central Universities under Grant (N2004011).

CONFLICT OF INTEREST

The authors declare that there are no conflicts of interest related to this paper.

DATA AVAILABILITY STATEMENT

Data sharing is not applicable to this article as no new data were created or analyzed in this study.

ORCID

Xuegang Li https://orcid.org/0000-0002-7894-6483

REFERENCES

[1] K. C. Kao, G. A. Hockham, *Electromagn. Wave Theory* **1967**, *113*(3), 441.
[2] U. S. Dinish, F. Beffara, G. Humbert, J.-L. Auguste, M. Olivo, *J. Biophoton.* **2019**, *12*(11), e201900027.
[3] A. Leal-Junior, A. Frizera, C. Marques, *Sensors* **2020**, *20*(11), 3026.
[4] N. H. Zainuddin, H. Y. Chee, M. Z. Ahmad, M. A. Mahdi, M. H. Abu Bakar, M. H. Yaacob, *J. Biophoton.* **2018**, *11*(8), e201700363.
[5] A. R. A. Rashid, A. A. N. Hakim, N. Yahaya, A. H. Surani, *Optoelectron. Adv. Mater.-Rapid Commun.* **2020**, *14*(3-4), 118.
[6] R. Srinivasan, S. Umesh, S. Murali, S. Asokan, S. S. Gorthi, *J. Biophoton.* **2017**, *10*(2), 224.
[7] K. D. Babu, P. Philominathan, K. Murali, *J. Mater. Sci.: Mater. Electron.* **2020**, *27*(5), 1.
[8] R. Ji, J. Liu, M.-M. Zhang, Y.-Y. Li, X.-L. Zuo, X. Wang, Y.-Q. Li, *Dig. Liver Dis.* **2020**, *52*(6), 651.
[9] C. Brown, D. Tseng, P. M. K. Larkin, S. Realegeno, A. Ozcan, *ACS Photonics* **2020**, *7*, 2527.
[10] J. Wang, K. Liu, Q. Sun, X. Ni, F. Ai, S. Wang, Z. Yan, D. Liu, *J. Biophoton.* **2019**, *12*(10), e201900084.
[11] R. Tabassum, S. K. Mishra, B. D. Gupta, *Phys. Chem. Chem. Phys.* **2013**, *15*(28), 11868.
[12] S. K. Mishra, S. N. Tripathi, V. Choudhary, B. D. Gupta, *Sens. Actuators, B* **2014**, *199*, 190.
[13] C. Zhou, H. K. Zhang, P. Song, J. Wang, C. G. Zhu, P. P. Wang, F. Peng, *IEEE Photon. Technol. Lett.* **2018**, *30*(23), 2037.
[14] H. Agrawal, A. M. Shrivastav, B. D. Gupta, *Sens. Actuators, B* **2016**, *227*, 204.
[15] R. Verma, B. D. Gupta, *Analyst* **2014**, *139*(6), 1449.
[16] S. P. Usha, A. M. Shrivastav, B. D. Gupta, *Biosens. Bioelectron.* **2016**, *85*, 986.

[17] P. Gong, X. Li, X. Zhou, Y. Zhang, N. Chen, S. Wang, S. Zhang, Y. Zhao, *Opt. Laser Technol.* **2021**, *139*, 106981.

[18] N. Chen, X. Zhou, X. Li, *IEEE Trans. Instrum. Meas.* **2021**, *70*, 1.

[19] A. Aray, F. Chiavaioli, M. Arjmand, C. Trono, S. Tombelli, A. Giannetti, N. Cennamo, M. Soltanolkotabi, L. Zeni, F. Baldini, *J. Biophoton.* **2016**, *9*(10), 1077.

[20] A. Bertucci, A. Manicardi, A. Candiani, S. Giannetti, A. Cucinotta, G. Spoto, M. Konstantaki, S. Pissadakis, S. Selleri, R. Corradini, *Biosens. Bioelectron.* **2015**, *63*, 248.

[21] X. Fang, C. R. Liao, D. N. Wang, *(in English), Opt. Lett.* **2010**, *35*(7), 1007.

[22] Y. Ma, X. Qiao, T. Guo, R. Wang, J. Zhang, Y. Weng, Q. Rong, M. Hu, Z. Feng, *(in English), Opt. Lett.* **2012**, *37*(3), 323.

[23] Y. Zhao, X. G. Hu, S. Hu, Y. Peng, *Biosens. Bioelectron.* **2020**, *166*, 112447.

[24] K. Chethana, A. S. Guru Prasad, S. N. Omkar, S. Asokan, *J. Biophoton.* **2017**, *10*(2), 278.

[25] S. Sridevi, K. S. Vasu, S. Sampath, S. Asokan, A. K. Sood, *J. Biophoton.* **2016**, *9*(7), 760.

[26] H. M. R. Goncalves, L. Moreira, L. Pereira, P. Jorge, C. Gouvei, P. Martins-Lopesac, J. R. A. Fernandes, *Biosens. Bioelectron.* **2016**, *84*, 30.

[27] X. Li, L. V. Nguyen, K. Hill, H. Ebendorff-Heidepriem, E. P. Schartner, Y. Zhao, X. Zhou, Y. Zhang, S. C. Warren-Smith, *Sens. Actuators, B* **2020**, *323*, 128681.

[28] X. Li, L. V. Nguyen, M. Becker, H. Ebendorff-Heidepriem, D. Pham, S. C. Warren-Smith, *IEEE J. Sel. Top. Quantum Electron.* **2020**, *26*(4), 1.

[29] X. Li, S. C. Warren-Smith, H. Ebendorff-Heidepriem, Y. Zhang, L. V. Nguyen, *J. Lightwave Technol.* **2019**, *37*(13), 2954.

[30] X. Li, S. C. Warren-Smith, L. Xie, H. Ebendorff-Heidepriem, L. V. Nguyen, *IEEE Sens. J.* **2020**, *20*(12), 6408.

[31] Y. S. Muanenda, C. J. Oton, F. D. Pasquale, *Front. Phys.* **2019**, *7*(155), 1.

[32] Y.-N. Zhang, S. E. B. Tao, Q. Wu, B. Han, *IEEE Trans. Instrum. Meas.* **2019**, *68*(11), 4566.

[33] Q. Wang, J.-Y. Jing, B.-T. Wang, *IEEE Trans. Instrum. Meas.* **2019**, *68*(9), 3350.

[34] H. Yuan, W. Ji, S. Chu, Q. Liu, J. Guang, G. Sun, Y. Zhang, X. Han, J.-F. Masson, W. Peng, *Biosens. Bioelectron.* **2020**, *154*, 112039.

[35] Y. Zhao, R.-j. Tong, F. Xia, Y. Peng, *Biosens. Bioelectron.* **2019**, *142*, 111505.

[36] M. Smietana, M. Koba, P. Sezemsky, K. Szot-Karpińska, D. Burnat, V. Stranak, J. Niedziółka-Jönsson, R. Bogdanowicz, *Biosens. Bioelectron.* **2020**, *154*, 112050.

[37] Q. L. Wu, Y. Zhao, Y. N. Zhang, S. X. Liu, Q. Zhao, S. Z. Chen, *Opt. Fiber Technol.* **2019**, *47*, 133.

[38] P. Li, H. Yan, Z. Xie, X. Zhao, D. Han, *Opt. Fiber Technol.* **2019**, *53*, 101998.

[39] Y. Huang, P. Chen, H. Liang, A. Xiao, B. O. Guan, *Biosens. Bioelectron.* **2020**, *156*, 112147.

[40] B. Gu, M. J. Yin, A. P. Zhang, J. W. Qian, S. He, *Opt. Express* **2009**, *17*(25), 22296.

[41] R. Kumar, Y. Leng, B. Liu, L. S. JunZhou, J. Yuan, X. Fan, S. Wan, T. Wu, J. Liu, R. Binns, Y. Q. Fu, W. P. Ng, G. Farrell, Y. Semenova, H. Xu, Y. Xiong, X. He, Q. Wu, *Biosens. Bioelectron.* **2019**, *145*, 111563.

[42] Samian, A. H. Zaidan, M. P. Anggraeni, M. Yasin, Supadi, *Microwave Opt. Technol. Lett.* **2019**, *61*(1), 223.

[43] P. Zhang, X. Tian, J. Zhang, *J. Phys. Conf.* **2020**, *1486*, 072041.

[44] M. J. Erro, A. Loayssa, S. Tainta, R. Hernandez, D. Benito, M. J. Garde, M. A. Muriel, *IEEE Trans. Instrum. Meas.* **2011**, *60*(4), 1416.

[45] J. Zhou, Y. Wang, C. Liao, B. Sun, J. He, G. Yin, S. Liu, Z. Li, G. Wang, X. Zhong, J. Zhao, *Sens. Actuators, B* **2015**, *208*, 315.

[46] T. Wei, J. Huang, X. Lan, Q. Han, H. Xiao, *Opt. Lett.* **2012**, *37*(4), 647.

[47] D. Wang, X. Cui, H. Zhang, *Opt. Lett.* **2020**, *45*(3), 726.

[48] Y. Dong, C. Sun, H. Xiao, C. Dong, S. Jian, *Opt. Fiber Technol.* **2017**, *33*, 39.

[49] S.-i. Takeda, Y. Aoki, Y. Nagao, *Compos. Struct.* **2012**, *94*(3), 813.

[50] F. Pang, W. Liang, W. Xiang, N. Chen, X. Zeng, Z. Chen, T. Wang, *IEEE Photon. Technol. Lett.* **2009**, *21*(2), 76.

[51] T. Gong, N. Zhang, K. V. Kong, D. Goh, C. Ying, J. L. Auguste, P. P. Shum, L. Wei, G. Humbert, K. T. Yong, M. Olivo, *J. Biophoton.* **2016**, *9*(1–2), 32.

[52] N. Edavalath, M. C. Günendi, R. Beravat, G. K. L. Wong, M. H. Frosz, J.-M. Ménard, P. S. J. Russell, *Opt. Lett.* **2017**, *42*(11), 2074.

[53] Y. Xu, X. Bao, *Can. J. Phys.* **2017**, *96*(4), 359.

[54] S. Choi, D. K. Kim, J. Kim, S.-L. Lee, M. S. Kim, Y. W. Lee, *Sens. Mater.* **2020**, *32*(2), 745.

[55] S. J. Kilic, Y. P. Zhu, Q. W. Sheng, M. N. Inci, M. Han, *Appl. Phys. B: Lasers Opt.* **2019**, *31*(8), 575.

[56] T. Young, *Philos. T. R. Soc. Lond.* **1805**, *95*, 65.

[57] P. Kozma, F. Kehl, E. Ehrentreich-Forster, C. Stamm, F. F. Bier, *Biosens. Bioelectron.* **2014**, *58*, 287.

[58] L. Singh, R. Singh, S. Kumar, B. Zhang, B. K. Kaushik, *IEEE J. Quantum Electron.* **2020**, *99*, 1.

[59] Y. Huang, Z. Tian, L. P. Sun, D. Sun, J. Li, Y. Ran, B. O. Guan, *Opt. Express* **2015**, *23*(21), 26962.

[60] B. Song, H. Zhang, B. Liu, W. Lin, J. Wu, *Biosens. Bioelectron.* **2016**, *81*, 151.

[61] M. Ding, Y. Huang, T. Guo, L. P. Sun, B. O. Guan, *Opt. Express* **2016**, *24*(24), 27152.

[62] M. Arjmand, H. Saghafifar, M. Alijanianzadeh, M. Soltanolkotabi, *Sens. Actuators, B* **2017**, *249*, 523.

[63] Y. Li, H. Ma, L. Gan, A. Gong, H. Zhang, D. Liu, Q. Sun, *J. Biophoton.* **2018**, *11*(9), 12.

[64] H. Abdullah, S. A. Mitu, K. Ahmed, *J. Electron. Mater.* **2020**, *49*, 4969.

[65] R. Kostecki, H. Ebendorff-Heidepriem, C. Davis, G. Mcadam, S. C. Warren-Smith, T. M. Monro, *Opt. Mater. Express* **2012**, *2*(11), 1538.

[66] Y. Zhao, X. Liu, R. Q. Lv, Y. N. Zhang, Q. Wang, *J. Lightwave Technol.* **2017**, *35*(16), 3406.

[67] E. P. Schartner, G. Tsiminis, A. François, R. Kostecki, S. C. Warren-Smith, L. V. Nguyen, S. Heng, T. Reynolds, E. Klantsataya, K. J. Rowland, A. D. Abell, H. Ebendorff-Heidepriem, T. M. Monro, *Int. J. Appl. Glass Sci.* **2015**, *6*(3), 1.

[68] J. Hu, D. Fu, C. Xia, S. Long, C. Lu, W. Sun, Y. Liu, *Appl. Opt.* **2019**, *58*(17), 4806.

[69] V. P. Minkovich, A. B. Sotsky, *J. Eur. Opt. Soc.-Rapid Publ.* **2019**, *15*(7), 1.

[70] L. V. Nguyen, K. Hill, S. Warren-Smith, T. Monro, *Sens. Actuators, B* **2015**, *221*, 320.
[71] M. J. Yin, C. Wu, L. Y. Shao, W. K. E. Chan, A. P. Zhang, C. Lu, H. Y. Tam, *Analyst* **2013**, *138*(7), 1988.
[72] W. Yu, T. Lang, J. Bian, W. Kong, *Sens. Actuators, B* **2016**, *228*, 322.
[73] J.-M. Hsu, J.-S. Horng, C.-L. Hsu, C.-L. Lee, *Opt. Commun.* **2014**, *331*, 348.
[74] S. Min, H. Liang, Z. Xue, F. Haiwei, *Acta Opt. Sin.* **2018**, *38*(3), 0328021.
[75] Z. Liuchao, J. Yi, J. Jingshan, W. Peng, W. Sumei, J. Lan, *Opt. Lasers Eng.* **2018**, *110*, 207.
[76] Y. Li, H. Ma, L. Gan, Q. Liu, Z. Yan, D. Liu, Q. Sun, *Sens. Actuators, B* **2018**, *255*, 3004.
[77] P. Sandhu, Y. Jian, X. Chang-Qing, *IEEE J. Sel. Top. Quantum Electron.* **2010**, *16*(3), 685.
[78] R. Gao, D. F. Lu, J. Cheng, Y. Jiang, L. Jiang, J. D. Xu, Z. M. Qi, *Biosens. Bioelectron.* **2016**, *86*, 321.
[79] K. Wysokinski, D. Budnicki, J. Fidelus, Ł. Szostkiewicz, Ł. Ostrowski, M. Murawski, M. S. MarcinStaniszewski, M. Napierała, T. Nasiłowski, *Biosens. Bioelectron.* **2018**, *114*, 22.
[80] L. Sun, J. Li, Y. Tan, X. Shen, X. Xie, S. Gao, B. O. Guan, *Opt. Express* **2012**, *20*(9), 10180.
[81] Z. Song, M. Guo, Q. Wang, *Microwave Opt. Technol. Lett.* **2017**, *59*(9), 2132.
[82] S. Gao, L. P. Sun, J. Li, L. Jin, Y. Ran, Y. Huang, B. O. Guan, *Opt. Express* **2017**, *25*(12), 13305.
[83] X. Z. Wang, Q. Wang, *Sensors (Basel)* **2018**, *18*(12), 4114.
[84] G. An, S. Li, Y. An, H. Wang, X. Zhang, *Opt. Commun.* **2017**, *405*, 143.
[85] S. C. Warren-Smith, R. Kostecki, L. V. Nguyen, T. M. Monro, *Opt. Express* **2014**, *22*(24), 29493.
[86] X. Li, L. V. Nguyen, Y. Zhao, H. Ebendorff-Heidepriem, S. C. Warren-Smith, *Sens. Actuators, B* **2018**, *269*, 103.
[87] P. G. Cielo, *Appl. Opt.* **1979**, *18*(17), 2933.
[88] F. Chen, Y. Jiang, H. Gao, L. Jiang, *Opt. Lasers Eng.* **2015**, *71*, 62.
[89] S. C. Warren-Smith, R. M. André, J. Dellith, T. Eschrich, M. Becker, H. Bartelt, *Sens. Actuators, B* **2017**, *244*, 1016.
[90] C. Wu, Z. Liu, A. P. Zhang, B. O. Guan, H. Y. Tam, *Opt. Express* **2014**, *22*(18), 21757.
[91] L. Xie, L. V. Nguyen, H. Ebendorff-Heidepriem, S. Warren-Smith, *IEEE Sens. J.* **2019**, *19*(22), 10425.
[92] D. Jauregui-Vazquez, J. M. Estudillo-Ayala, R. Rojas-Laguna, E. Vargas-Rodríguez, J. M. Sierra-Hernández, J. C. Hernández-García, R. I. Mata-Chávez, *Sensors (Basel)* **2013**, *13*(5), 6355.
[93] X. H. Liu, M. S. Jiang, Q. M. Sui, S. Y. Luo, X. Y. Geng, *Opt. Fiber Technol.* **2016**, *30*, 32.
[94] Y. Zhang, H. Shibru, K. L. Cooper, A. Wang, *Opt. Lett.* **2005**, *30*(9), 1021.
[95] L. H. Chen, C. C. Chan, R. Menon, P. Balamurali, W. C. Wong, X. M. Ang, P. B. Hu, M. Shaillender, B. Neu, P. Zu, Z. Q. Tou, C. L. Poh, K. C. Leong, *Sens. Actuators, B* **2013**, *188*, 185.
[96] Y. Yuan, X. Yang, D. Gong, F. Liu, W. Hu, W. Cai, J. Huang, M. Yang, *Opt. Express* **2017**, *25*(4), 3884.
[97] Y. C. Chung, Y. C. Lin, C. D. Chueh, C. Y. Ye, L. W. Lai, Q. Zhao, *Electrophoresis* **2008**, *29*, 1859.
[98] J. B. Fiche, A. Buhot, R. Calemczuk, T. Livache, *Biophys. J.* **2007**, *92*(3), 935.

SUPPORTING INFORMATION

Additional supporting information may be found online in the Supporting Information section at the end of this article.

How to cite this article: Li X, Chen N, Zhou X, et al. A review of specialty fiber biosensors based on interferometer configuration. *J. Biophotonics*. 2021;e202100068. https://doi.org/10.1002/jbio.202100068